

1 **Tetratricopeptide repeat domain 36 protects renal**
2 **tubular cells from cisplatin-induced apoptosis via**
3 **maintaining mitochondrial homeostasis**

4
5 **Xin Yan¹, Rui Peng¹, Dayu Tian¹, Lei Chen¹, Qingling He¹, Qianyin Li^{1, *} and**
6 **Qin Zhou^{1, *}**

7 ¹ The Ministry of Education Key Laboratory of Clinical Diagnostics, School of
8 Laboratory Medicine, Chongqing Medical University, Chongqing 400016, China;

9 * Correspondence: zhouqin@cqmu.edu.cn (Q.Z.) or liqianyin904@cqmu.edu.cn

10 (Q.L.); Tel.: +86-23-6378-6981

11
12
13
14
15

16 **TTC36 inhibits cisplatin-induced apoptosis**

17
18
19
20

21 **Keywords:** Acute kidney injury, ischemia/reperfusion, apoptosis, TTC36,
22 mitochondria, cisplatin

23
24
25
26
27
28
29
30

31 **Abstract**

32 The apoptosis of proximal tubule epithelial cells (PTECs) is a critical event of
33 acute kidney injury (AKI). Tetratricopeptide repeat domain 36 (TTC36) with three
34 tetratricopeptide repeats is evolutionarily conserved across mammals, which functions
35 as a chaperone for heat shock protein 70. We have revealed that TTC36 is specifically
36 expressed in PTECs in our previous work. There are few studies about the role TTC36
37 played in AKI. Therefore, in this study, we investigated the function of TTC36 in the
38 apoptosis of HK2 cells, which are derived from the human proximal tubule. Firstly, we
39 observed that TTC36 was obviously down-regulated and was negatively related to the
40 kidney damage degree in a mouse model of acute kidney injury established by
41 ischemia/reperfusion. In addition, TTC36 overexpression protected HK2 cells against
42 cisplatin-induced apoptosis. Moreover, we discovered the mechanism that TTC36
43 mitigated cisplatin-triggered mitochondrial disorder via sustaining the membrane
44 potential of mitochondria and mitochondrial autophagy-related gene expression.
45 Collectively, these results suggested that TTC36 plays a protective role in the cisplatin-
46 induced apoptosis of renal tubular cells through maintaining the mitochondrial potential
47 and mitochondrial autophagy-related gene expression. These observations highlight the
48 essential role of TTC36 in regulating PTEC apoptosis and imply TTC36/mitochondrial
49 homeostasis axis as a potential target for the therapeutic intervention in AKI.

50 **Introduction**

51 Acute kidney injury (AKI), with the characteristic of the rapid decline of
52 glomerular filtration rate (GRF), is a worldwide clinical syndrome accompanied by the
53 sudden increase of serum creatinine (SCr) and blood urea (BUN)(1,2). AKI, primarily
54 caused by ischemia, sepsis, and nephrotoxicity, not only leads to approximately 1.7
55 million deaths every year but also makes patients prone to chronic kidney disease
56 (CKD)(1,3,4). However, there is still no efficient remedy for curing AKI. Therefore, it
57 is necessary to investigate the underlying mechanisms of AKI and excavate the
58 potential strategy for the prevention and treatment of AKI.

59 During the progression of AKI, the dysfunction and apoptosis of proximal tubular

60 epithelial cells, which are intensively packed with mitochondria, are regarded as a key
61 event(5). Synthesizing adenosine 5'-triphosphate (ATP) via electron transport and
62 oxidative phosphorylation (OXPHOS) in concert with the oxidation of metabolites by
63 the tricarboxylic acid cycle and catabolism of fatty acids by β -oxidation,
64 mitochondria play a critical role in supporting cellular energy-intensive processes,
65 including generating ion gradients and reabsorbing ions(6-8). Adjusted by mitophagy,
66 autophagy-related clearance of impaired mitochondria, mitochondrial biogenesis and
67 mitochondrial dynamics, mitochondrial homeostasis are vital for cellular homeostasis
68 and function(9). However, the disorder of mitochondrial homeostasis and the damage
69 of PTECs' integrity could contribute to energy metabolism falling apart, which finally
70 facilitates or even leads to AKI(10-12). Given the significance of mitochondria in
71 energy homeostasis, it is a potential and promising strategy that mitigating AKI via
72 targeting mitochondrial metabolism.

73 Tetratricopeptide repeat domain 36 (TTC36) is a conserved protein with three
74 tetrapeptide repeats, which serves as a chaperone of heat shock protein 70. TTC36
75 primarily expressed in liver and renal proximal tubular epithelial cells in kidneys(13).
76 Current studies have observed that it participates in the metabolism of tyrosine by
77 interacting with 4-hydroxyphenylpyruvic acid dioxygenase (HPD) and reducing the
78 binding of serine/threonine kinase 33 (STK33) to HPD to block the degradation of HPD
79 in hepatocyte(14). It is worth noting that TTC36 is restrictively expressed in renal
80 proximal tubules in kidney. However, there is no research revealing the role of TTC36
81 in acute kidney injury.

82 In this study, we employed HK2 cells, which are derived from human proximal
83 tubule, and established an animal model to uncover the role of TTC36 in AKI. We
84 revealed that TTC36 protects HK2 cells against cisplatin-induced apoptosis via
85 maintaining mitochondrial membrane potential and mitochondrial autophagy-related
86 gene expression, implying a promising access to treat AKI.

87 **Materials and Methods**

88 *Materials*

89 Rabbit polyclonal antibody anti-TTC36 was made in previous work(15). Mouse

90 anti-Bcl2 (sc-7382), anti-Bax (sc-20067), and anti-Phospho-Bcl2 (sc-293128) were
91 purchased from Santa Cruz Biotechnology (Santa Cruz, CA, USA). Rabbit antibodies
92 against Caspase-3 (9662S) and Caspase-9 (9502S) were obtained from Cell Signaling
93 Technology (Danvers, MA, USA). Mouse anti-Flag (AE005) and anti-GAPDH (AC002)
94 were obtained from Abclonal (Wuhan, China). Mouse anti- β -Actin (HC201) was
95 obtained from TransGen Biotech (Beijing, China). JC-1 (HY-15534), Cisplatin (CP)
96 (HY-17394) were obtained from MedChemExpress (New Jersey, USA). For
97 Immunohistochemical (IHC) staining, SP kit (SP-9001) and Diaminobenzidine (DAB)
98 coloring kit (ZLI-9017) were purchased from ZSGB-BIO (Beijing, China). Serum
99 creatinine (SCr) detection Kit (C011-2-1) and blood urea nitrogen (BUN) detection kit
100 (C013-2-1) were obtained from Nanjing Jiancheng Bioengineering Institute (Nanjing,
101 China).

102 ***DNA Construction***

103 To construct the overexpression vector of *TTC36*, human *TTC36*
104 (NM_001080441.4) was amplified with cDNA and subcloned into the CMV vector.

105 ***Mice and AKI model***

106 All animals were reared under the condition of a standard laboratory where food
107 and water were sufficiently supplied. 8-week-old male wild-type (WT) C57BL/6 mice
108 were obtained from the Laboratory Animal Centre of Chongqing Medical University
109 (No. SYXK2018-0003, Chongqing, China). *Ttc36* knockout (*Ttc36*^{-/-}) mice were
110 generated in previous work(16), these mice develop normally with a normal lifespan
111 even though they will suffer from Hypertyrosinemia when 8-12 month-old. A total of
112 22 mice were used in this study, including 19 WT and 3 *Ttc36*^{-/-} C57BL/6 mice. To
113 evaluate the correlation of TTC36 expression with renal function, 8-week-old male WT
114 C57BL/6 mice were assigned to 4 groups (Sham, n = 4; 2 days after IR-treated, n = 4;
115 7 days after IR-treated, n=4; 14 days after IR-treated, n=4). For the isolation of primary
116 renal tubular epithelial cells, 8-week-old male WT and *Ttc36*^{-/-} C57BL/6 mice were
117 sacrificed (WT mice, n = 3; *Ttc36*^{-/-} mice, n = 3). All animal related experiments were
118 approved by Animal Ethical Commission of Chongqing Medical University. The mice
119 were anesthetized with ether and warmed by a heating pad at 37.0 °C during the surgery.

120 To establish the acute kidney injury, bilateral renal arteries were separated and were
121 clamped for 30 min(17). In the sham group, the mice were treated with the same way
122 except arteries clamping. Mice were euthanized by cervical dislocation after
123 anesthetized with ether, then the blood were collected for the detection of SCr and BUN
124 and kidneys were obtained for Hematoxylin-Eosin (HE) staining,
125 immunohistochemical (IHC) staining, mRNA quantification, and western blotting.

126 ***Cell culture and treatment***

127 HK2 cells, which derived from the human proximal tubule, were cultured in
128 Dulbecco's modified Eagle's medium-F12 (DMEM/F12) medium (Gibco)
129 supplemented with 10% fetal bovine serum (Biological Industries) and 1% penicillin-
130 streptomycin (HyClone). The HEK293T cells, packaging cells, were maintained in
131 DMEM medium (Gibco) containing 10% fetal bovine serum (Biological Industries)
132 and 1% penicillin-streptomycin (Gibco). To construct TTC36 stably overexpressed
133 cells, HEK293T cells were transfected with TTC36 overexpression vectors and
134 lentivirus backbone vectors using TurboFect™ Transfection Reagent (ThermoFisher
135 Scientific). Then, for the enrichment of lentivirus, the supernatant were collected and
136 purified by ultra-high-speed centrifugation (25,000 × g for 2h at 4°C) after transfection
137 for 48h. HK2 cells were infected with lentivirus using 8 µg/mL polybrene (Sigma). To
138 select the stable clones, HK2 cells were treated with puromycin (Invitrogen). To knock
139 down the expression of TTC36, si-RNA for silencing TTC36 (si-TTC36, sequence 5'-
140 GGAAGAACGAGAAGAAGAUGA-3') were synthesized by GenePharma (Jiangsu,
141 China), and transfected into HK2 cells with Lipofectamine 2000 Transfection Reagent
142 (ThermoFisher Scientific) according to the manual. In order to establish the in vitro
143 model of AKI, HK2 cells were treated with a series concentration of cisplatin, then we
144 used 25µM cisplatin to treat HK2 cells for 20 hours to induce acute tubular injury.

145 ***Isolation of Mouse Primary Renal Tubular Cells***

146 Primary renal tubular cells were isolated from 8-week-old wild type and *Ttc36*^{-/-}
147 C57BL/6 mice. In Brief, after starved overnight, the mice were anesthetized with ether
148 and their kidneys was perfused with 20 mL perfusion buffer (1% penicillin-
149 streptomycin (HyClone) in PBS) through the left ventricle and then perfused with 30

150 mL digestion buffer (0.13 mg/mL collagenase type II (Sigma), Hank's balanced salt
151 solution (HyClone) with 5 mM Ca^{2+} and 1.2 mM Mg^{2+}). After perfused, the kidneys
152 were removed from the abdominal cavity. After the renal capsules and medulla were
153 removed, the cortex was cut into tiny pieces and incubated with digestion buffer at
154 37 °C for 10 min. The tubular cells were collected using filters followed by centrifuging
155 at 50×g for 5 min. After that, cells were suspended, transferred into collagen type I
156 coated 100 mm dishes (coating buffer, 4% collagen type I (Corning) and 0.2% glacial
157 acetic acid in PBS), and cultured in DMEM/F12 (Gibco) medium containing 20%
158 FBS(Gibco) and 1% penicillin-streptomycin (HyClone).

159 ***Hematoxylin and Eosin (H&E) Staining and IHC Staining***

160 The kidneys were harvested, fixed in 4% formaldehyde, embedded in paraffin, and
161 cut into 4 μm sections. To process the H&E staining, have dewaxed and rehydrated, the
162 sections were stained with hematoxylin (2 min), soaked with acid alcohol (2 sec),
163 soaked in lithium carbonate (2 min) and 80% ethanol (1 min) in sequence, and
164 counterstained with eosin for 1min. For IHC staining, after pre-heated at 65°C for 2h,
165 the sections were dewaxed and rehydrated, heated at 100°C for 20min in the presence
166 of citric acid buffer (pH = 6.0) to retrieve antigen, placed at room temperature for 4h to
167 cool down, treated with hydrogen-peroxide-solution for 10min, coated with goat serum
168 for blocking, incubated with the antibody at 4°C for overnight, washed with PBST(0.05%
169 Tween20 in PBS)for three times, coated with appropriate secondary antibody labeled
170 with biotin for 15min, incubated with streptavidin-conjugated with horseradish
171 peroxidase (HRP) at room temperature for 15min. After that, the sections were stained
172 using a DAB coloring kit.

173 ***Western Blotting***

174 Cells were lysed with lysis buffer (50 mM Tris–HCl pH 7.5, 1% SDS, 1% TritonX-
175 100,150 mM NaCl, 1 mM dithiothreitol, 0.5 mM EDTA, 100 mM PMSF, 100 mM
176 leupeptin, 1 mM aprotinin, 100 mM sodium orthovanadate, 100 mM sodium
177 pyrophosphate, and 1 mM sodium fluoride) after rinsed three times with cold PBS, then
178 the extraction were collected to 1.5 ml microtube and heated at 95 °C in mental bath
179 (ThermoFisher Scientific) for 10 min. After that, the protein was centrifuged at

180 10,000×g for 10 min and quantified by BCA Protein Assay Kit (Thermo Fisher
181 Scientific). The same quantity (about 15 µg) protein of each sample was separated with
182 12% sodium dodecyl sulfate-polyacrylamide gel and transferred to polyvinylidene
183 difluoride membranes (Millipore). After blocked by 5% fat-free milk (Sangon Biotech)
184 in Tris-buffered saline containing 0.08% Tween 20 (Sigma) at room temperature for 2h,
185 the membranes were incubated with primary antibodies at 4°C overnight, washed three
186 times with TBST, 10min each, incubated with appropriate secondary antibodies coupled
187 with HRP for 1 hour at room temperature, and washed with TBST again. The target
188 bands were detected with Smart-ECL basic (Smart-Lifesciences) using Image Lab
189 software program (Bio-Rad). Actin or GAPDH was used for the loading control. For
190 the detection of Bcl2 and p-Bcl2, the PVDF membranes were first incubated with anti-
191 p-Bcl2 antibody to detect it, then these PVDF membranes were washed with stripping
192 buffer to stripe the bands and incubated with anti-Bcl2 antibodies after blocked with 5%
193 fat-free milk. For integral optical density analysis, the bands were scanned and
194 calculated by Image J software.

195 ***Mitochondrial Membrane Potential Assay***

196 The membrane potential ($\Delta\Psi_m$) of mitochondrial was determined by JC-1 which
197 is a fluorescent dye and can selectively enter mitochondria. In brief, when the $\Delta\Psi_m$ is
198 relatively low, JC-1 forms monomers and emits green fluorescence. On the contrary,
199 when the $\Delta\Psi_m$ is high, it will aggregate and transmit red fluorescence. After treatment,
200 HK2 cells were incubated with JC-1 according to the manual, and detected by a
201 CytoFLEX flow cytometry (BECKMAN COULTER)

202 ***Cell Viability Assay***

203 After treated with cisplatin, the cell viability assay was performed using methyl
204 thiazolyl tetrazolium (MTT). Briefly, cells were cultured in a 96-well plate, and each
205 well was added 20 µl 5 mg/ml MTT, incubated at 37°C for 4 h. Then, the medium was
206 discarded and each well was added 150 µl dimethylsulfoxide (DMSO), shaking at low
207 speed for 10 min, and determined with MULTISKAN GO (ThermoFisher Scientific) at
208 OD 490 nm.

209 ***Apoptosis Assay***

210 Cells undergoing apoptosis were quantitatively determined with Annexin V PE/7-
211 AAD kit (Solarbio). Digested with trypsin and washed with PBS for three times, cells
212 were incubated with the reagent according to the manufacturer's instructions, and
213 detected with CytoFLEX flow cytometry (BECKMAN COULTER).

214 ***Quantitative Real-Time Polymerase Chain Reaction (RT-qPCR)***

215 For the detection of specific gene's mRNA expression level in HK2 cells and
216 kidney tissue, cells or tissue were lysed with TRIzol reagent (Invitrogen). The total
217 RNA was extracted using chloroform and isopropanol, washed with 75% ethyl alcohol,
218 and dissolved with DNase/RNase-free water (Solarbio). To perform RT-qPCR, the total
219 RNA was used for synthesizing cDNA with RevertAid RT Reverse Transcription Kit
220 (Thermo Fisher scientific) under the guidance of manufacturer's instructions. After that,
221 the cDNA library was amplified in the presence of specific primers and 2x SYBR Green
222 qPCR Master Mix (bimake) with a CFX96 real-time PCR detection system (Bio-Rad).
223 The relative expression level of specific genes was analyzed relative to the mean critical
224 threshold (CT) values of the 18S gene. Primer sequences of specific genes were listed
225 in Supplementary Table S1.

226 ***Statistical Analyses***

227 All experiments were repeated independently three times. Data were exhibited as
228 mean \pm standard deviation using GraphPad Prism 8 software, and the Statistically
229 significant differences were calculated by analysis of variance (ANOVA), followed by
230 a Student's *t*-test using IBM SPSS Statistics 20 software. Differences were regarded as
231 significant with $p < 0.05$. * $p < 0.05$, ** $p < 0.01$, *** $p < 0.001$, and **** $p < 0.0001$.

232 **Results**

233 ***The reduction of TTC36 expression in murine renal tubular cells was related to AKI***

234 First, we established the in vivo model of AKI with the bilateral renal artery and
235 vein clamping for 30 minutes, as shown in Fig. 1A. Next, we detected the concentration
236 of serum creatinine (SCr) and blood urea nitrogen (BUN) in mice at the indicated time,
237 and an apparent increasement of SCr and BUN were observed in IR-treated mice after
238 2 days compared to those in the Sham group (Fig. 1, B and C). At the same time, a

239 significant reduction of TTC36 expression was detected in kidneys from mice with IRI,
240 and recovery of TTC36 expression along with the decrease of SCr and BUN
241 concentration was found (Fig. 1, B to E).

242

243 ***The expression of TTC36 was negatively correlated with the degree of kidney injury***

244 In line with the above data, an obvious renal tubular injury accompanied by the
245 downregulation of TTC36 expression was confirmed in histological staining (Fig. 2, A
246 and B). Further analysis demonstrated that the expression of TTC36 in tubular cells was
247 negatively correlated with the concentrations of SCr ($r = -0.7224, p < 0.0001$) and BUN
248 ($r = -0.6870, p < 0.001$) (Fig. 2 C and D), suggesting that the down-regulation of TTC36
249 is associated with the pathogenesis of acute tubular injury.

250

251 ***Overexpression of TTC36 protected renal tubular cells against cisplatin-induced*** 252 ***apoptosis***

253 To further elucidate the role of TTC36 in AKI, proximal tubular cells (HK2) were
254 treated with cisplatin as an in vitro model of acute tubular injury. Consistent with in
255 vivo results, overexpression of TTC36 augmented the viability and survival of HK2
256 cells which were subjected to cisplatin treatment (Fig. 3, A, B, and C). The expression
257 of BCL-2, an integral outer mitochondrial membrane protein that inhibits the cellular
258 apoptotic death, was increased, and the expression of BAX, which functions as an
259 apoptotic activator, was decreased in TTC36 overexpressed HK2 cells (Fig. 3, D and E).
260 Consistently, in primary tubular cells isolated from *Ttc36*^{-/-} mice kidneys, the
261 expression of BCL-2 was down-regulated whereas the expression of BAX was up-
262 regulated in comparison to those derived from WT mice (Fig. 3F). Furthermore, the
263 overexpression of TTC36 down-regulated cleaved Caspase-9 and cleaved Caspase-3
264 expression and reduced the increment of those in cisplatin-induced HK2 cells,
265 compared to control group (Fig. 3G). Coincident with the above data, an evident up-
266 regulation of cleaved Caspase-9 expression was observed after TTC36 was silenced
267 (Fig. 3H). In conclusion, these results demonstrated that TTC36 overexpression was
268 beneficial to renal tubular cells against cisplatin-induced apoptosis.

269

270 ***TTC36 mitigated cisplatin-induced mitochondrial dysfunction***

271 The homeostasis of mitochondria is critical for the survival and function of renal
272 tubular cells in AKI. We further investigated the effect of *TTC36* on mitochondrial
273 membrane potential (MMP) maintenance in cisplatin-induced tubular cell injury using
274 JC-1, which is a MMP indicator that forms aggregate and emits red fluorescence in
275 relatively high MMP. As shown in Fig. 4, A and B, the MMP was reduced in cisplatin-
276 treated cells and partially reversed by the overexpression of *TTC36*. Mitophagy and
277 proper mitochondrial dynamics are vital for normal mitochondrial function. The
278 expression of *MFN1*, *MFN2*, and *OPA1*, which indicate the fusion of
279 mitochondria(18,19), was rescued by *TTC36* overexpressing in cisplatin-treated HK2
280 cells, compared to the CP-treated control group (Fig. 4C). Based on the importance of
281 mitophagy clearance for mitochondrial homeostasis, we examined expression of
282 mitophagy-related genes in cisplatin-treated HK2 cells and observed that
283 overexpression of *TTC36* alleviated the reduction of *ATG5*, *ATG7*, *PARKN*, and
284 *BNIP3L* expression (Fig. 4D), which are responsible for the regulation of
285 mitophagy(20-23). The decreased expression of *PPARGCIA*, *SOD2*, and *NFE2L2*,
286 which play a protective role in mitochondria(24-27) in cisplatin-treated HK2 cells, was
287 ameliorated by *TTC36* overexpressing (Fig. 4E). Collectively, these results suggested
288 that *TTC36* plays a protective role in cisplatin-induced mitochondrial dysfunction via
289 maintaining mitophagy clearance and mitochondrial dynamics.

290

291

292 **Discussion**

293 It has been demonstrated that the specific expression of *TTC36* in renal proximal
294 tubular cells in our previous work(15). However, no study has been performed to
295 uncover the role of *TTC36* in AKI. We conducted these experiments with genetic and
296 pharmacological methods to revealed the role *TTC36* played during the pathogenesis
297 of acute renal damage. Here, we demonstrated the pathogenic impact of *TTC36*
298 deficiency in acute renal tubular damage and mitochondrial disorder in vitro.

299 Overexpression of TTC36 effectively mitigated mitochondrial disorder and inhibited
300 cell apoptosis induced by cisplatin. All these experimental data suggested the function
301 of TTC36 in maintaining mitochondrial homeostasis, facilitating the protection for
302 kidneys in acute injury.

303 It is considered that the main victims in AKI, including cisplatin-induced
304 nephrotoxicity, are renal tubular cells, which are full of mitochondria(28). The latter
305 are anticipated to be the primary objects in acute tubular cell injury, featured with the
306 reduction of MMP and OCR and the impairment of mitophagy and fatty acid-
307 oxidation(10). In consistence with the above opinion, many studies focusing on
308 maintaining the homeostasis of mitochondrial to improve AKI have been
309 performed(29-31). Here, we revealed that the indicators related to mitochondrial
310 function and homeostasis, containing the MMP, the expression of mitochondria-related
311 genes, and mitophagy were partially promoted by TTC36 overexpression in cisplatin-
312 treated HK2 cells, suggesting that TTC36 mitigate cisplatin-induced mitochondria
313 dysfunction.

314 As a pathological phenomenon and a pathogenic factor, Mitochondrial
315 dysfunction contributes to a serious of harmful reactions, including oxidative stress,
316 inflammation, and tubular cell damage and apoptosis(32,33). Mitochondria, which are
317 in charge of producing a dominant portion of cellular energy in the shape of ATP, are
318 considered as vital organelles of eukaryotic cells, including ROS level regulation,
319 buffering cytosolic calcium, and apoptosis regulation, and those are closely related to
320 the pathophysiology of diseases(34). Mitochondria contain bilayer membranes where
321 the inner membrane in charge of mitochondrial oxidative phosphorylation and the outer
322 membrane consisting of crucial proteins associated with the regulation of apoptosis.
323 We observed that TTC36 protected HK2 cells against apoptosis in an in vitro model of
324 cisplatin-induced acute tubular injury. However, to reveal the detailed mechanism of
325 TTC36 in regulating cell apoptosis, there are still lots of attempts need to perform in
326 the future.

327 The limitation of our research is that the role of TTC36 in apoptosis and
328 mitochondrial homeostasis was observed in cultured cells instead of human tissue. We

329 revealed that the down-regulation of TTC36 is negatively correlated with the degree of
330 renal injury in vivo model of IR-induced AKI, however, the usefulness and significance
331 of TTC36 in protecting AKI patients still need further investigations using patient
332 specimens and clinical trials of TTC36 agonist in the future.

333 **Conclusions**

334 In this study, we first discovered that TTC36 overexpression protected HK2 cells
335 against cisplatin-induced apoptosis via maintaining mitochondrial homeostasis in the
336 aspect of mitochondrial membrane potential and mitophagy-related gene expression.
337 These findings uncovered in our study not only augment our understanding of the
338 molecular mechanism and pathogenesis of AKI but also imply that developing safe and
339 effective agonists of TTC36 could be a potential therapeutic strategy for AKI patients.

340 **Disclosure statement**

341 The authors declare no conflict of interest.

342 **Funding statement**

343 This research was funded by the National Natural Science Foundation of China
344 (grant number 81873932 and 81802549) and by the technology innovation and
345 application development special key projects of Chongqing province (grant number
346 cstc2019jscx-dxwtBX0032).

347 **Supplementary Material**

348 Supplementary Table S1

349 **References**

- 350 1. Bello, A., Alrukhaimi, M., Ashuntantang, G., Bellorin-Font, E., Benghanem Gharbi, M.,
351 Braam, B., Feehally, J., Harris, D., Jha, V., Jindal, K., Johnson, D., Kalantar-Zadeh, K.,
352 Kazancioglu, R., Kerr, P., Lunney, M., Olanrewaju, T., Osman, M., Perl, J., Rashid, H., Rateb,
353 A., Rondeau, E., Sakajiki, A., Samimi, A., Sola, L., Tchokhanelidze, I., Wiebe, N., Yang, C., Ye,
354 F., Zemchenkov, A., Zhao, M., and Levin, A. (2018) Global overview of health systems
355 oversight and financing for kidney care. *Kidney international supplements* **8**, 41-51
- 356 2. Gonzalez, S., Cortês, A., Silva, R., Lowe, J., Prieto, M., and Silva Lara, L. (2019) Acute kidney
357 injury overview: From basic findings to new prevention and therapy strategies.
358 *Pharmacology & therapeutics* **200**, 1-12
- 359 3. Rewa, O., and Bagshaw, S. M. (2014) Acute kidney injury-epidemiology, outcomes and
360 economics. *Nature Reviews Nephrology* **10**, 193-207

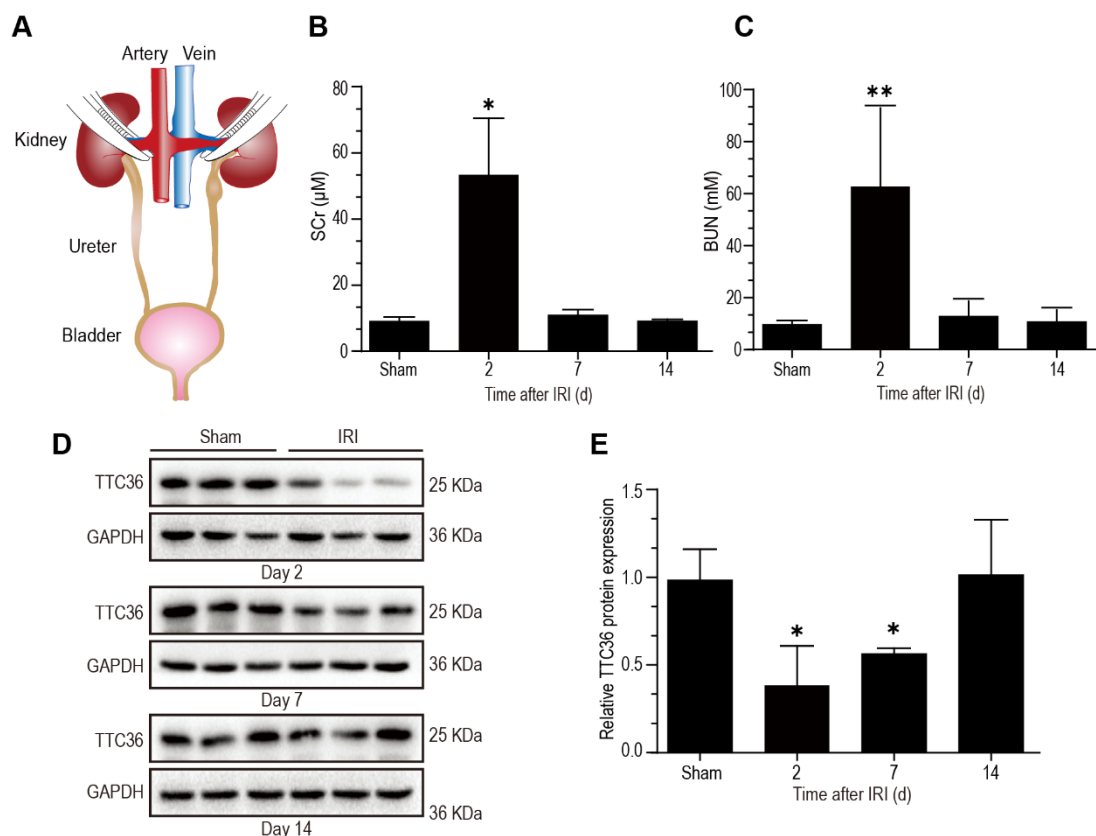
- 361 4. Makris, K., and Spanou, L. (2016) Acute Kidney Injury: Definition, Pathophysiology and
362 Clinical Phenotypes. *Clinical Biochemist Reviews* **37**, 85
- 363 5. Tang, C., Cai, J., Yin, X., Weinberg, J., Venkatachalam, M., and Dong, Z. (2020)
364 Mitochondrial quality control in kidney injury and repair. *Nature reviews. Nephrology*
- 365 6. Soltoff, and P, S. (1986) ATP and the Regulation of Renal Cell Function. *Annual Review of*
366 *Physiology* **48**, 9
- 367 7. Eloot, S., Schepers, E., Barreto, D. V., Barreto, F. C., Liabeuf, S., Van Biesen, W., Verbeke, F.,
368 Glorieux, G., Choukroun, G., and Massy, Z. (2011) Estimated Glomerular Filtration Rate Is
369 a Poor Predictor of Concentration for a Broad Range of Uremic Toxins. *Clinical Journal of*
370 *the American Society of Nephrology Cjasn* **6**, 1266
- 371 8. Sun, J., Zhang, J., Tian, J., Virzì, G., Digvijay, K., Cueto, L., Yin, Y., Rosner, M., and Ronco, C.
372 (2019) Mitochondria in Sepsis-Induced AKI. *Journal of the American Society of*
373 *Nephrology : JASN* **30**, 1151-1161
- 374 9. Ploumi, C., Daskalaki, I., and Tavernarakis, N. (2016) Mitochondrial biogenesis and
375 clearance: a balancing act. *Febs Journal* **284**
- 376 10. Hall, A. M., and Schuh, C. D. (2016) Mitochondria as therapeutic targets in acute kidney
377 injury. *Current Opinion in Nephrology & Hypertension* **25**, 355
- 378 11. Bhargava, P., and Schnellmann, R. G. (2017) Mitochondrial energetics in the kidney. *Nature*
379 *Reviews Nephrology*
- 380 12. Szeto, and Hazel, H. (2017) Pharmacologic Approaches to Improve Mitochondrial
381 Function in AKI and CKD. *Journal of the American Society of Nephrology,*
382 *ASN.2017030247*
- 383 13. Zhou, Y., He, Q., Chen, J., Liu, Y., Mao, Z., Lyu, Z., Ni, D., Long, Y., Ju, P., Liu, J., Gu, Y., and
384 Zhou, Q. (2016) The expression patterns of Tetratricopeptide repeat domain 36 (Ttc36).
385 *Gene Expr Patterns* **22**, 37-45
- 386 14. Xie, Y., Lv, X., Ni, D., Liu, J., Hu, Y., Liu, Y., Liu, Y., Liu, R., Zhao, H., Lu, Z., and Zhou, Q. (2019)
387 HPD degradation regulated by the TTC36-STK33-PELI1 signaling axis induces tyrosinemia
388 and neurological damage. *Nat Commun* **10**, 4266
- 389 15. Yuru, Zhou, Qingling, He, Jihui, Chen, Yunhong, Liu, Zhaomin, and Mao. (2016) The
390 expression patterns of Tetratricopeptide repeat domain 36 (Ttc36). *Gene Expression*
391 *Patterns*
- 392 16. Liu, Y., Lv, X., Tan, R., Liu, T., Chen, T., Li, M., Liu, Y., Nie, F., Wang, X., and Zhou, P. (2014)
393 A Modified TALEN-Based Strategy for Rapidly and Efficiently Generating Knockout Mice
394 for Kidney Development Studies. *Plos One* **9**
- 395 17. Wang, D. B., Uo, T., Kinoshita, C., Sopher, B. L., Lee, R. J., Murphy, S. P., Kinoshita, Y., Garden,
396 G. A., Wang, H. G., and Morrison, R. S. (2014) Bax interacting factor-1 promotes survival
397 and mitochondrial elongation in neurons. *The Journal of neuroscience : the official journal*
398 *of the Society for Neuroscience* **34**, 2674-2683
- 399 18. Cao, Y., Meng, S., Chen, Y., Feng, J., Gu, D., Yu, B., Li, Y., Yang, J., Liao, S., Chan, D., and
400 Gao, S. (2017) MFN1 structures reveal nucleotide-triggered dimerization critical for
401 mitochondrial fusion. *Nature* **542**, 372-376
- 402 19. Song, Z., Chen, H., Fiket, M., Alexander, C., and Chan, D. (2007) OPA1 processing controls
403 mitochondrial fusion and is regulated by mRNA splicing, membrane potential, and Yme1L.
404 *The Journal of cell biology* **178**, 749-755

- 405 20. Wang, Y., Zhu, J., Liu, Z., Shu, S., Fu, Y., Liu, Y., Cai, J., Tang, C., Liu, Y., Yin, X., and Dong, Z.
406 (2020) The PINK1/PARK2/optineurin pathway of mitophagy is activated for protection in
407 septic acute kidney injury. *Redox biology* **38**, 101767
- 408 21. Mai, S., Muster, B., Bereiter-Hahn, J., and Jendrach, M. (2012) Autophagy proteins LC3B,
409 ATG5 and ATG12 participate in quality control after mitochondrial damage and influence
410 lifespan. *Autophagy* **8**, 47-62
- 411 22. Xiong, J. (2015) Atg7 in development and disease: panacea or Pandora's Box? *Protein &*
412 *cell* **6**, 722-734
- 413 23. Kitamura, N., Nakamura, Y., Miyamoto, Y., Miyamoto, T., Kabu, K., Yoshida, M., Futamura,
414 M., Ichinose, S., and Arakawa, H. (2011) Mieap, a p53-inducible protein, controls
415 mitochondrial quality by repairing or eliminating unhealthy mitochondria. *Plos One* **6**,
416 e16060
- 417 24. Fujita, H., Fujishima, H., Chida, S., Takahashi, K., Qi, Z., Kanetsuna, Y., Breyer, M. D., Harris,
418 R. C., Yamada, Y., and Takahashi, T. (2009) Reduction of Renal Superoxide Dismutase in
419 Progressive Diabetic Nephropathy. *Journal of the American Society of Nephrology* **20**,
420 1303-1313
- 421 25. Gureev, A. P., and Popov, V. N. (2019) Nrf2/ARE Pathway as a Therapeutic Target for the
422 Treatment of Parkinson Diseases. *Neurochemical Research*
- 423 26. Sharma, S., Bhattarai, S., Ara, H., Sun, G., St Clair, D., Bhuiyan, M., Kevil, C., Watts, M.,
424 Dominic, P., Shimizu, T., McCarthy, K., Sun, H., Panchatcharam, M., and Miriyala, S. (2020)
425 SOD2 deficiency in cardiomyocytes defines defective mitochondrial bioenergetics as a
426 cause of lethal dilated cardiomyopathy. *Redox biology* **37**, 101740
- 427 27. Tran, M., Tam, D., Bardia, A., Bhasin, M., Rowe, G., Kher, A., Zsengeller, Z., Akhavan-Sharif,
428 M., Khankin, E., Saintgeniez, M., David, S., Burstein, D., Karumanchi, S., Stillman, I., Arany,
429 Z., and Parikh, S. (2011) PGC-1 α promotes recovery after acute kidney injury during
430 systemic inflammation in mice. *The Journal of clinical investigation* **121**, 4003-4014
- 431 28. Manohar, S., and Leung, N. (2017) Cisplatin nephrotoxicity: a review of the literature.
432 *Journal of Nephrology*
- 433 29. Liu, D., Shu, G., Jin, F., Qi, J., Xu, X., Du, Y., Yu, H., Wang, J., Sun, M., You, Y., Zhu, M., Chen,
434 M., Zhu, L., Shen, Q., Ying, X., Lou, X., Jiang, S., and Du, Y. (2020) ROS-responsive chitosan-
435 SS31 prodrug for AKI therapy via rapid distribution in the kidney and long-term retention
436 in the renal tubule. *Science advances* **6**
- 437 30. Liu, D., Jin, F., Shu, G., Xu, X., Qi, J., Kang, X., Yu, H., Lu, K., Jiang, S., Han, F., You, J., Du, Y.,
438 and Ji, J. (2019) Enhanced efficiency of mitochondria-targeted peptide SS-31 for acute
439 kidney injury by pH-responsive and AKI-kidney targeted nanopolyplexes. *Biomaterials*
440 **211**, 57-67
- 441 31. Fu, Z., Wang, Z., Xu, L., Chen, X., Li, X., Liao, W., Ma, H., Jiang, M., Xu, T., Xu, J., Shen, Y.,
442 Song, B., Gao, P., Han, W., and Zhang, W. (2020) HIF-1 α -BNIP3-mediated mitophagy in
443 tubular cells protects against renal ischemia/reperfusion injury. *Redox biology* **36**, 101671
- 444 32. Emma, F., Montini, G., Parikh, S. M., and Salviati, L. (2016) Mitochondrial dysfunction in
445 inherited renal disease and acute kidney injury. *Nature Reviews Nephrology* **12**, 267-280
- 446 33. Yu, I., and Reiko, I. Mitochondria: a therapeutic target in acute kidney injury. *Nephrology,*
447 *dialysis, transplantation : official publication of the European Dialysis and Transplant*
448 *Association - European Renal Association*, 1062

449 34. Wallace, D. C. (2005) A mitochondrial paradigm of metabolic and degenerative diseases,
 450 aging, and cancer: a dawn for evolutionary medicine. *Annual review of genetics* **39**, 359-
 451 407

452
 453
 454
 455

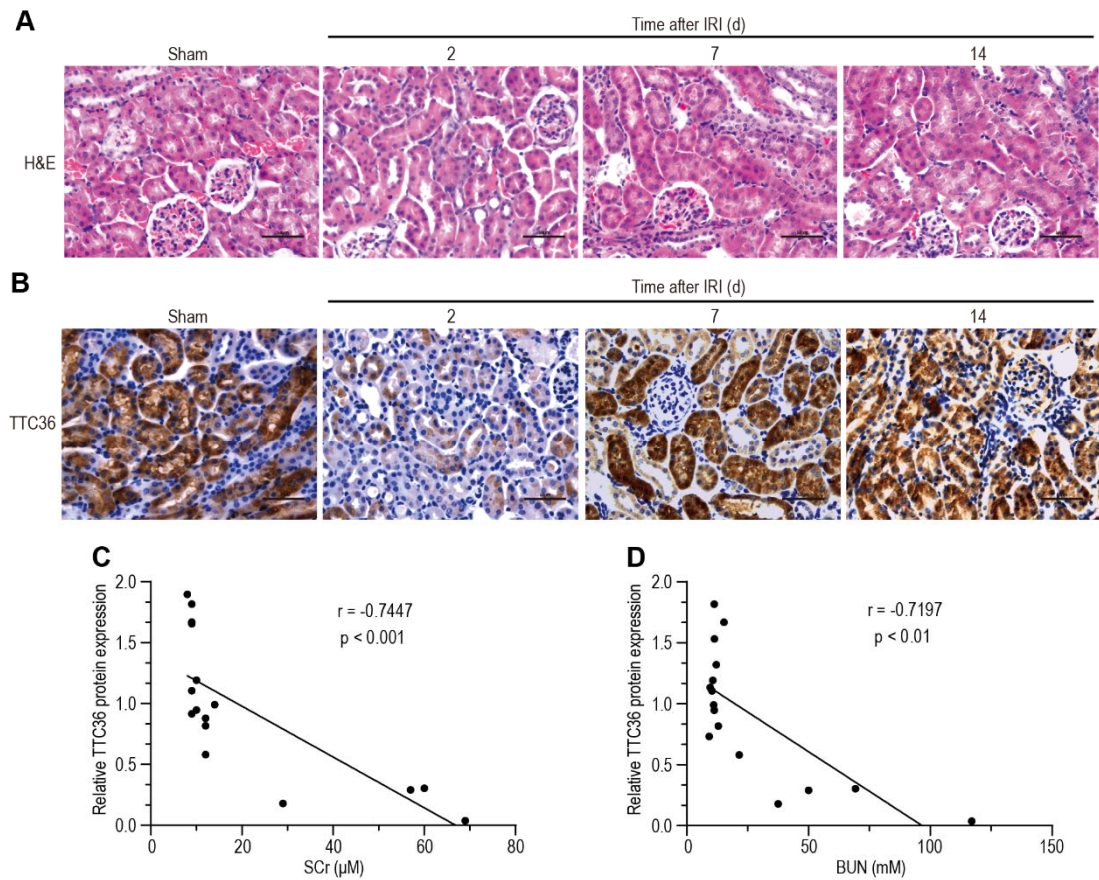
Figure 1



456

457 **Figure 1. The reduction of TTC36 expression in murine renal tubular cells was related to AKI.** (A) surgery
 458 strategy of IR to induce AKI. (B) the Concentration of SCr in IR-induced mice (Sham and 2, 7 and 14 days after
 459 IR-treatment; n=4 mice per group). (C) the Concentration of BUN in IR-induced mice (Sham and 2, 7 and 14 days
 460 after IR-treatment; n=4 mice per group). (D) Western blotting for TTC36 in the kidneys of IR-treated mice (Sham,
 461 2, 7 and 14 days after IR-treatment; n = 3 mice per group). (E) Quantitative analysis of the TTC36 expression related
 462 to GAPDH through detecting the integral optical density of (D). Data are expressed as means \pm SD. Statistically
 463 significant differences were determined by Student's *t*-test and one-way ANOVA. **p* < 0.05 and ***p* < 0.01 versus
 464 Sham group. Results are representative of at least three independent experiments. SCr, serum creatinine; IR,
 465 ischemia/reperfusion; BUN, blood urea nitrogen; TTC36, tetratricopeptide repeat domain 36; GAPDH,
 466 glyceraldehyde-phosphate dehydrogenase; AKI, acute kidney injury; SD, standard deviation; ANOVA, analysis of
 467 variance.

468 **Figure 2**



469

470 **Figure 2. The Expression of TTC36 Was Negatively Correlated with The Degree of Kidney Injury. (A)**

471 Representative images of hematoxylin-eosin staining in the kidneys of IR-treated mice (Sham and 2, 7 and 14 days

472 after IR-treatment; n = 3 mice per group; scale bars, 50 μ m). (B) Representative images of immunohistochemical

473 staining of TTC36 in the kidneys of IR-treated mice (Sham and 2, 7 and 14 days after IR-treatment; n = 3 mice per

474 group; scale bars, 50 μ m). (C) Correlation between renal TTC36 expression and the concentration of SCr in IR-

475 induced mice (Sham and 2, 7 and 14 days after IR-treatment; n=4 mice per group). (D) Correlation between renal

476 TTC36 expression and the concentration of BUN in IR-induced mice (Sham and 2, 7 and 14 days after IR-treatment;

477 n=4 mice per group). Statistically significant differences were determined by Student's t-test and one-way ANOVA.

478 SCr, serum creatinine; BUN, blood urea nitrogen; IR, ischemia/reperfusion; ANOVA, analysis of variance. H&E,

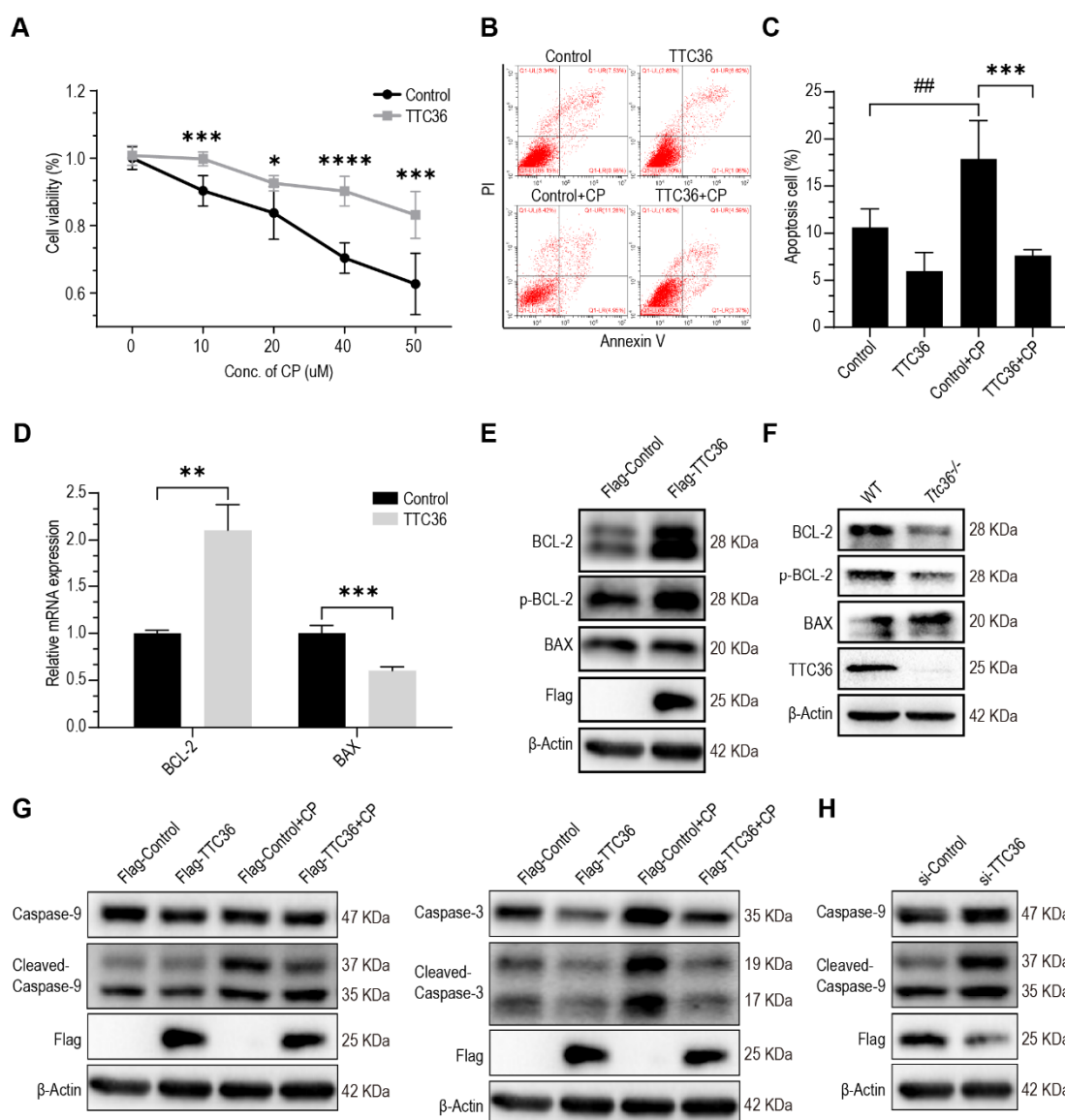
479 Hematoxylin-Eosin.

480

481

482

483 **Figure 3**



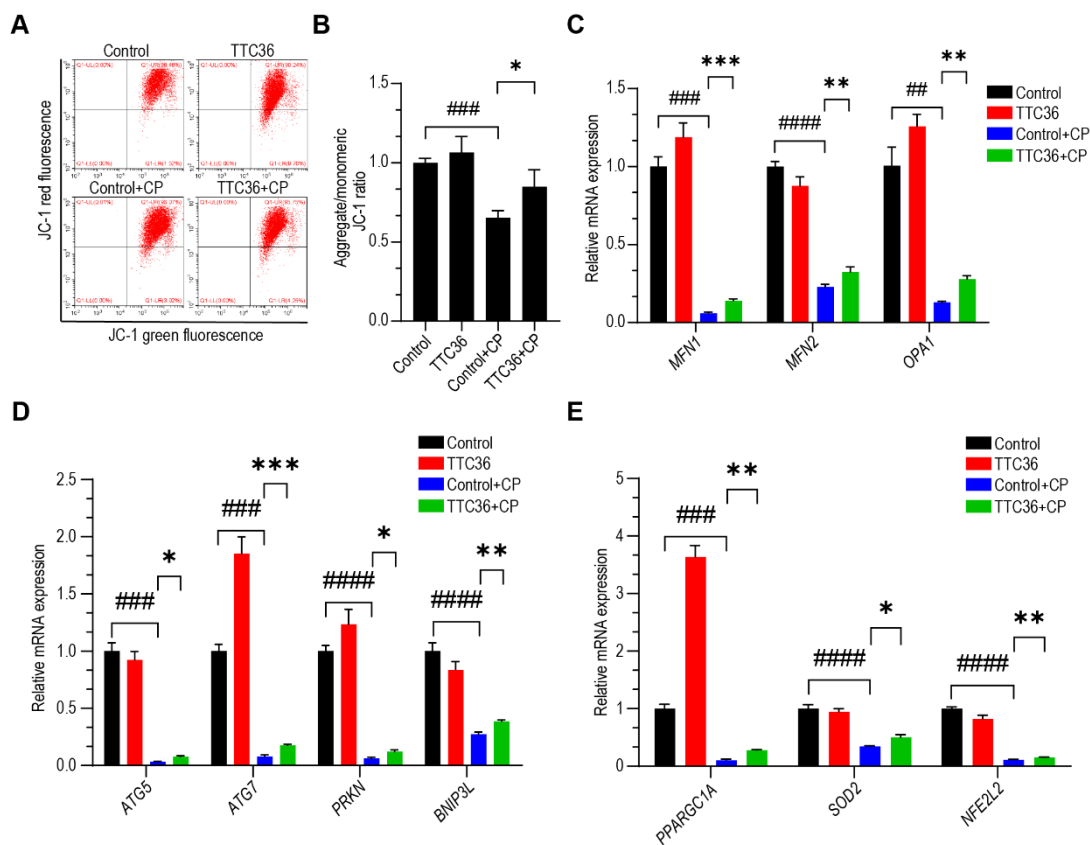
484
 485 **Figure 3. TTC36 overexpressing protected renal tubular cells against cisplatin-induced apoptosis.** (A) The
 486 viability of HK2 cells with or without TTC36 overexpression were assayed with MTT after they were treated with
 487 indicated concentration of CP for 20 hours. (B) Representative images for FACS analysis after annexin V and PI
 488 staining. TTC36 was overexpressed in HK2 cells followed by treatment with 25 μM CP for 20 hours. (C)
 489 Quantitative analysis for the percentages of apoptosis cells with FACS. (D) The relative mRNA expression of *BCL*-
 490 2 and *BAX* were analyzed using RT-qPCR. 18s was used as an internal control. (E) Western blotting for Flag-tagged
 491 TTC36, BAX, BCL2, and p-BCL2 in HK2 cells overexpressed with TTC36, β-Actin as a loading control. Bcl2 was
 492 detected following p-Bcl2 being stripped with stripping buffer. (F) Western blotting for TTC36, BAX, BCL2, and
 493 p-BCL2 in isolated primary tubular cells of WT and *Tic36*^{-/-} mice. Bcl2 was detected after p-Bcl2 being stripped.
 494 (G) Western blotting for caspase-9, cleaved caspase-9, casepase-3, cleaved caspase-3, and Flag-tagged TTC36 in
 495 CP-treated HK2 cells with or without TTC36 overexpression. Caspase-9 and casepase-3 were detected in two gels.
 496 (H) Western blotting for Flag-tagged TTC36, caspase-9 and cleaved caspase-9 in CP-treated overexpressed with
 497 TTC36 HK2 cells with or without TTC36 silenced. Data are shown as means ± SD (n = 3). Statistically significant
 498 differences were determined by Student's *t*-test and one-way ANOVA. **p* < 0.05, ***p* < 0.01, ****p* < 0.001, and
 499 *****p* < 0.0001. Results are representative of at least three independent experiments. CP, cisplatin; TTC36,
 500 tetratricopeptide repeat domain 36; BCL-2, BCL2 apoptosis regulator; BAX, BCL2 associated X, apoptosis
 501 regulator; p-BCL2, phosphorylated-BCL2 apoptosis regulator; MTT, methyl thiazolyl tetrazolium; FACS,

502 fluorescence-activated cell sorting; PI, propidium iodide; RT-qPCR, quantitative real-time PCR; ANOVA, analysis
 503 of variance.

504

505

506 **Figure 4**



507

508 **Figure 4. TTC36 mitigated cisplatin-induced mitochondrial dysfunction.** (A) Representative images for FACS

509 analysis after HK2 cells were incubated with CP (25 μ M) for 20 hours followed by JC-1. (B) The ratios of JC-1 red

510 fluorescence to JC-1 green fluorescence in CP-induced HK2 cells were quantified using FACS. (C) RT-qPCR

511 analyses for *MFN1*, *MFN2*, and *OPA1* mRNA expressions. (D) The relative mRNA expressions of *ATG5*, *ATG7*,

512 *PRKN*, and *BNIP3L* were analyzed by RT-qPCR. (E) RT-qPCR analyses for *PPARGC1A*, *SOD2*, and *NFE2L2*

513 mRNA expressions. Data are shown as means \pm SD (n = 3). Statistically significant differences were determined by

514 Student's *t*-test and one-way ANOVA. **p* < 0.05, ***p* < 0.01, ****p* < 0.001, and *****p* < 0.0001. Results are

515 representative of at least three independent experiments. *MFN1*, mitofusin 1; *MFN2*, mitofusin 2; *OPA1*, OPA1

516 mitochondrial dynamin like GTPase; CP, cisplatin; *ATG5*, autophagy related 5; *ATG7*, autophagy related 7; *PRKN*,

517 parkin RBR E3 ubiquitin protein ligase; *BNIP3L*, BCL2 interacting protein 3 like; *PPARGC1A*, PPARG coactivator

518 1 alpha; *SOD2*, superoxide dismutase 2; *NFE2L2*, nuclear factor, erythroid 2 like 2; FACS, fluorescence-activated

519 cell sorting; CP, cisplatin; RT-qPCR, quantitative real-time PCR; ANOVA, analysis of variance.